

Table 1 Thermal balances from second test

Heat load	Ergometer setting, K_p	
	1.5	1.0
Heat generated (Btu/hr):		
Metabolic output (Q_{met})	1655	1080
Body heat loss (Q_{stor})	0	167
	1655	1247
Heat removed (Btu/hr):		
Sensible (Q_s)	149	121
Latent (Q_l)	1292	956
Loss to ambient ($Q_r + Q_c$)	-50	-50
Mechanical work (Q_{mech})	250	167
	1641	1194

chosen as a realistic theoretical outlet temperature based on experimental data. Curve *C* represents the test data; the vertical line through each data point represents the estimated error range. Comparison of Curve *C* to Curve *A* at 4 cfm indicates a ventilation efficiency of 58%. The thermal balances in Table 1 were established during the second test.

The ventilation flow rate remained constant at 4.1 cfm at STP. The heat loads removed by the stream ($Q_s + Q_l$) at 1.5 K_p work load and 1.0 K_p work load were 1441 and 1077 Btu/hr, respectively. The mean body temperature was 1.2°F higher at stabilization during the 1.5 K_p work load than during stabilization at 1.0 K_p work load. Excessive sweat, during the 1.5 K_p work-load period, "pooled" in the lower sections of the space suit and was relatively unavailable to the ventilation flow. The mean body temperature was steady during the stabilization period at 1.5 K_p work load and continued to decrease during the 1.0 K_p work load. From these limited results, it appears that the subject would have maintained an acceptable mean body temperature (within the physiological limitations of dehydration and fatigue) indefinitely when working at a 1.0 K_p load with a 4-cfm-at-STP ventilation flow rate, and that this flow rate probably is adequate for a 1.5 K_p work load. However, it must be noted that the Q_l 's measured correspond to the evaporation of approximately 0.9 to 1.3 lb/hr of body water, so that dehydration will result with prolonged work in the space suit. Hence, means for replacing lost water and electrolytes must be provided in the final design and included in the space suit's operational requirements.

Conclusion

Suited subjects at 35,000-ft simulated altitude, instrumented for electrocardiograms and rectal and skin temperatures, performed work satisfactorily on a bicycle ergometer at a constant metabolic rate (1500 Btu/hr) while the ventilation rate was successively increased from 2.5 to 5.8 cfm STP and at different metabolic rates (1080 and 1655 Btu/hr) while the ventilation rate was held constant at 4.1 cfm at STP. At a work load of 1.5 K_p on the ergometer, the total heat leaving the subject was calculated to be 1641 Btu/hr (sensible, 149; latent, 1292; mechanical, 250; convective and radiant, -50) compared to a metabolic generation rate (as indicated by CO_2 production) of 1655 Btu/hr. Results of the first test (Fig. 4) suggest that the heat removed by the ventilation stream would not be significantly increased by a flow rate greater than 4 cfm at STP, at which the ventilation efficiency was 58% for $Q_{met} = 1500$ Btu/hr. These limited data suggest that the suit ventilation is adequate for continuous work at the levels investigated, but that body dehydration would result from prolonged work in the suit.

References

- 1 Bard, P., *Medical Physiology* (C. V. Mosby and Co., St. Louis, Mo., 1956), p. 580.
- 2 Benjamin, F., personal communication, Office of Space Medicine, NASA Headquarters, Washington, D. C. (July 1964.)

Analytical Model to Determine Aft-End Igniter Design Parameters

ARNOLD G. PLUMLEY*

Aerojet General Corporation, Sacramento, Calif.

Nomenclature

A	= area, in. ²
a^*	= sonic velocity of igniter gas, fps
C_w	= flow coefficient = $(\gamma g/RT)^{0.5} [2/(\gamma + 1)] \times \exp(\gamma + 1)/2(\gamma - 1)$, sec ⁻¹
g	= earth gravitational acceleration, ft/sec ²
M	= Mach number
\dot{m}	= igniter mass flow rate, slugs/sec
P	= pressure, psia
$\int P dA$	= integrated pressure, area force of chamber gas on converging portion of motor exhaust nozzle, lbf
R	= gas constant, ft/ ^o R
T	= igniter gas total temperature, ^o R
V	= volume, ft ³
v	= velocity, fps
\dot{w}	= igniter flow rate, lb/sec
Γ	= $1 + (\gamma - 1)/2 M^2$
γ	= ratio of specific heats
ϵ^*	= ratio of minimum annular flow area between igniter and motor-exit cone to the motor throat area

Subscripts

e	= at motor throat plane for gas leaving motor chamber
i	= at motor throat plane for igniter gas entering motor chamber
ign	= igniter
p	= motor port
t	= motor throat
to	= total conditions
0	= at motor plane entering nozzle converging section for gas leaving motor chamber
1	= initial or ambient conditions
2	= pressurized conditions
s	= static conditions

Introduction

THE conventional igniter for a solid-propellant rocket motor generates hot gas, which impinges on the motor propellant and raises the motor chamber pressure. It is normally positioned in the forward end of the motor. An aft-end igniter is positioned near the motor throat and discharges its gas through the motor throat into the motor chamber. Design values for mass flow rate and operating pressure of the conventional igniter have been determined largely through testing. Such a trial-and-error procedure would be very costly on the 260-in.-diam motor. The analytical model described herein permits the sizing of aft-end igniters to obtain desired motor chamber pressure and igniter-gas penetration prior to propellant ignition. These design criteria are presented as functions of the pertinent motor and igniter parameters, and the equations are presented graphically for an igniter operating at 1000 psia. The analysis does not allow prediction of the over-all ignition transient, which will require more comprehensive treatment.

Analytical Model

The analytical model is based on the following two elementary concepts: 1) the incoming igniter gas expands to the static pressure in the motor throat and requires a portion of the throat flow area; the remaining flow area must be sufficient to allow the same flow out of the motor at the same static pressure at sonic velocity; and 2) the incoming flow must be turned around in order to flow out the motor; since

Received January 6, 1954; revision received March 30, 1965.

* Development Engineer; now with Chrysler Corp., Highland Park, Mich.

the motor free volume determines the pressure in the forward end of the motor, the over-all effect of the aft-end igniter gas can be determined without analyzing the intermediate non-isentropic processes of the actual flowfield.

It is assumed that 1) one-dimensional flow exists where flow is analyzed; 2) the igniter gases do not mix with the cold gas in the motor chamber, but rather compress the trapped gas isentropically ($PV^\gamma = \text{const}$); 3) the igniter gas expands isentropically to P_{st} in the motor throat plane; 4) the igniter-gas jet maintains the same size and velocity as determined by assumption 3 for a distance into the motor where the port area is uniform (station 2 in Fig. 1); this assumption causes an error of less than 1% for $P_2 < 140$ psia and $A_p/A_t > 1.3$; 5) the igniter gas entering the motor does not mix appreciably with the gas leaving the chamber; and 6) the flow is choked for the gases leaving the motor chamber. From continuity, and for choked flow in each direction

$$C_w P_{ign} A_{ign} = C_w P_{tot} A_e \quad (1)$$

Employing assumption 5,

$$A_t = A_i + A_e \quad (2)$$

The portion of the motor throat area that is blocked by the incoming igniter gases may be expressed by the relation:

$$\frac{A_i}{A_{ign}} = \frac{(2/\gamma + 1) \exp(\gamma + 1)/2(\gamma - 1)}{\left(\frac{P_{st}}{P_{ign}}\right)^{1/\gamma} \left\{ \left(\frac{2}{\gamma - 1}\right) \left[1 - \left(\frac{P_{st}}{P_{ign}}\right)^{(\gamma - 1)/\gamma} \right] \right\}^{0.5}} \quad (3)$$

For the condition of choked flow out the motor

$$P_{st} = [2/(\gamma + 1)]^{\gamma/(\gamma - 1)} P_{tot} \quad (4)$$

Considering momentum and forces as being positive when directed toward the left in Fig. 1, an equation for a control volume encompassing the entire motor chamber from the plane of the motor throat forward may be written as

$$\dot{m} v_e - (-\dot{m} v_i) = P_2 A_p - P_{st} A_t - \int P dA \quad (5)$$

Similarly for a second volume near the motor throat, using assumption 5:

$$\dot{m} v_e - \dot{m} v_0 = P_{tot} (A_p - A_i) \Gamma_0^{-\gamma/(\gamma - 1)} - P_{st} A_e - \int P dA \quad (6)$$

Next, the isentropic relationships between the velocities, area ratios, Mach numbers, and pressure ratios may be written for the incoming gas and the gas leaving the motor. These relationships are

$$v_i = a^* \{ M_i^2 \Gamma_i^{-1} (\gamma + 1)/2 \}^{0.5} \quad (7)$$

$$P_{ign}/P_{st} = \Gamma_i^{\gamma/(\gamma - 1)} \quad (8)$$

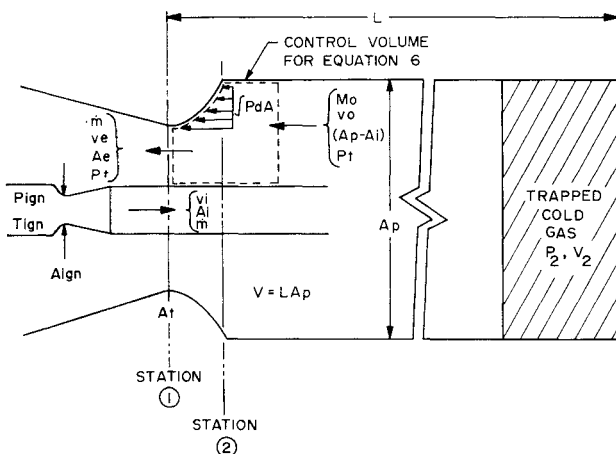


Fig. 1 Aft-end ignition system schematic diagram.

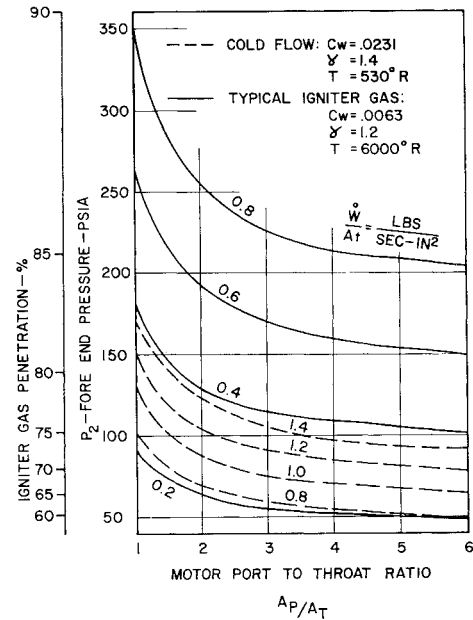


Fig. 2 Analytical model predicted chamber pressure and penetration plotted as function of igniter flow to motor throat and motor port to throat ratios.

$$v_0 = a^* \{ M_0^2 \Gamma_0^{-1} (\gamma + 1)/2 \}^{0.5} \quad (9)$$

$$(A_p - A_i)/A_e = \{ 2/(\gamma + 1) \} \exp(\gamma + 1)/2(\gamma - 1)$$

$$M_0^{-1} \Gamma_0 \exp(\gamma + 1)/2(\gamma - 1) \quad (10)$$

where a^* is the sonic velocity of the gas. Because the exhausting gas is choked at the motor throat, $v_e = a^*$. The solution of Eqs. (1-10) is presented graphically in Fig. 2 for an igniter operating at 1000 psia chamber pressure (for igniter pressures ordinarily of interest, i.e., 500 to 2000 psi, the curves are not affected appreciably by P_{ign}). The curves are presented for the igniter gas having properties of air and having those typical of solid propellants. The hot-gas penetration also is presented as a second ordinate for the corresponding motor chamber pressure using $PV^\gamma = \text{const}$, % penetration = $100 (V_1 - V_2)/V_1$. For $P_2 > 60$ psia, the change in hot-gas penetration is very small compared to the change in pressure. At 70 psia, for example, a 10% change in pressure changes the penetration by only about 3% of the motor length.

Cold-Flow Test Program

The igniter hardware consisted of converging-diverging nozzles connected to a regulated supply of dry nitrogen. Nozzles with throat diameters of 0.739, 0.64, and 0.522 in. were used. The motor chamber was simulated by a large tube into which wooden inserts were placed to simulate the motor bore and exhaust nozzle configurations. Two inserts were fabricated; both had a 3.09 in. throat and an exit-cone half angle of 17.5°, but cylindrical port areas differed to give $A_p/A_t = 3$ and 1.3, which correspond to the short and full length 260-in.-diam motor configurations. The igniter nozzle could be moved axially, but the annular flow area between the igniter and the motor exit cone was kept greater than A_t . The ratio of these areas is referred to as ϵ^* ; values of 1.3, 1.55, and 1.8 were used. This parameter was considered to be of primary importance by other investigators. Based on assumptions 3-5 of the analytical model, ϵ^* should not affect the chamber pressurization as long as it exceeds 1. Inlet igniter-gas pressures and temperatures were measured in the nitrogen gas supply tube, and pressure transducers were placed in the motor throat and at four axial stations along the motor chamber. The over-all accuracy is approximately ± 4 psi for the pressure data because of a 1% trans-

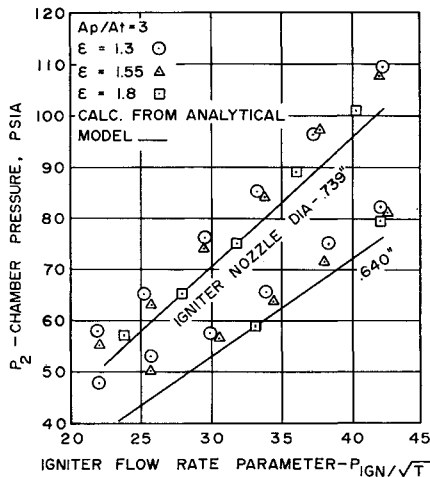


Fig. 3 Aft-end ignition cold-flow test data for motor port to throat of 3.

ducer calibration accuracy and about 3% for reading the oscillograph traces. For $P_2 > 65$ psia, the error in the analytical model compared to test data was +6% to -14% which corresponds to motor length penetration errors of approximately +2% to -4%, respectively. The analytically predicted pressures for $A_p/A_t = 3$ correlated better with the data than did those for $A_p/A_t = 1.3$, probably because the assumption of isentropic flow without viscous mixing is poorer for the latter case. This assumption also is amplified because of the physical size of the test hardware, where the mixing layer is larger relative to the jet size than it would be in the full size igniter and motor.

Conclusions

The analytical model is useful for sizing aft-end ignition systems with regard to motor pressurization and igniter-gas penetration. Figures 3 and 4 show the correlation of the analytical model to the test data. It is probable that the greatest cause of error in the analytical model is the assumption of no mixing. Jet mixing reduces the effective flow area in the motor throat which tends to make the pressures

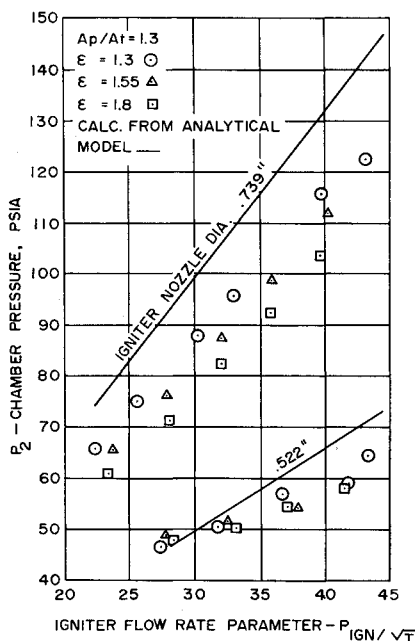


Fig. 4 Aft-end ignition cold-flow test data for motor port to throat ratio of 1.3.

higher; whereas, shredding off of the incoming jet stream would tend to reduce the incoming momentum and consequently lower the chamber pressure. Since these two effects are in opposition, the relative effects depend on the geometry and value of igniter-motor parameters. No attempts are made here to apply empirical corrections to the analytical model, since such corrections may not be scalable and may introduce errors greater than the assumptions. The error in the analytical model is less than the variation in chamber pressurization caused by igniter flow rate changes resulting from temperature variations of 60° to 100°F in ordinary solid propellants.

The axial position of the igniter (which controls ϵ^*) has relatively little effect on the motor pressurization for $1.3 < \epsilon^* < 1.8$; the only effect was a slight lowering of pressure at greater stand-off distances, probably due to the assumption that mixing did not occur between the igniter jet and the main gas stream. Pressure varied very little along the motor length; this lends credence to the conclusion that most of the igniter jet turning takes place in a relatively short distance inside the motor throat.

Saturn S-II Operations Development Progress

W. F. PARKER*

North American Aviation, Inc., Downey, Calif.

THE S-II is the second stage of the Saturn V launch vehicle. After separation of the S-IC first-stage engines, the S-II will, during its 395-sec burning time, increase the altitude of the S-IV-B and Apollo spacecraft from 200,000 to 600,000 ft and the velocity to 21,000 fps. The power to achieve this is provided by five Rocketdyne J-2 engines, each of which will have a thrust of 200,000 lb in vacuum, using LH_2 and LOX . The S-II (Fig. 1) is 33 ft in diameter and 81½ ft long, weighing approximately 90,200 lb empty and 1,071,000 lb loaded. The total propellant capacity is 970,000 lb. The stage structure follows the conventional semimonocoque design using 2014-T6 aluminum alloy for the greater part. The major portions of the S-II are occupied by the LH_2 tank forward and the LOX tank aft, whose volumes are 38,400 ft³ and 12,930 ft³, respectively. The two propellant tanks are separated by a "common" bulkhead that comprises a forward-facing sheet as the lower bulkhead of the LH_2 tank and an aft-facing sheet as the forward bulkhead of the LOX tank. These sheets are separated by and bonded to an insulating core composed of a phenolic honeycomb (which varies in thickness from 4.75 in. at the center to 0 at its outside edges) that prevents the LOX from being frozen by the LH_2 .

The LH_2 section comprises six cylindrical segments welded together at their peripheries to form a tank 56 ft long. Each cylindrical segment is composed of four curved sections. Prior to forming, these sections are machine milled to form a waffle pattern on the inside. The protrusions of this pattern, approximately ¼ in. thick with a depth of 1 in., provide for attachment of flanged tank frames. The LOX tank is a 33-ft-diam × 22-ft-high spheroid fabricated from ellipsoidal shaped upper and lower halves. The upper half is the "common" bulkhead already referred to. A J-section is welded to

Presented as Preprint 65-201 at the AIAA/NASA Flight Testing Conference, Huntsville, Ala., February 15-17, 1965; revision received April 9, 1965.

* Vice President and Program Manager, Saturn S-II, Space and Information Systems Division. Member AIAA.